Advances in Engineering Design Technology Vol. 3, 2021 pp. 115-131 ISSN-2682-5848

NIPES

Advances in Engineering Design Technology

Journal homepage: www.nipesjournals.org.ng

Simulation of Mass and Pressure Dynamics of In-Cylinder Charges at Variable Valve Lift Clearance in Four Stroke Spark Ignition Engine

Ikpe Aniekan Essienubong**, Owunna Ikechukwu Bismarck
Department of Mechanical Engineering, University of Benin, Benin City, Edo State, PMB 1154, Nigeria

ARTICLE INFORMATION

Keywords:
Valve lift, SI Engine, Four Stroke, In-Cylinder Charges, Charge pressure, Mass of Charge, Simulation

Received 28 Oct. 2021
Revised 22 November 2021
Accepted 25 November 2021
Available online 19 January 2022

https://doi.org/10.37933/nipes.a/3.2.2021.10
https://nipesjournals.org.ng

ABSTRACT

The performance of any given four stroke IC engine cycle is influenced by various parameters during service condition. SOLIDWORKS 2017 version was used to simulate the effect of different valve lift clearance (ranging from 5-13 mm) on the mass and pressure of in-cylinder charges in four stroke spark ignition engine speeds (ranging from 1000-12000 rpm). The study revealed that for simulation at a particular engine speed, more charges were ingested into the cylinder as the valve lift clearance increased. This led to effective combustion process, but can sometimes result in losses if the valve opening clearance is very wide. For example, at 12000 rpm, the 13mm valve lift showed a pressure of 1.12 *bar while the 5mm valve lift showed a pressure of* 0.89 *bar. Higher valve lift clearance led to increase in the quantity and mass of charge ingested into the engine cylinder, thus, more loses and vice versa. The mass intake was observed to reduce at higher engine speeds when compared to low speeds. This is because the engine piston moved very fast with intense heat (converting some charges into gas-vapour) requiring less time for charges in the intake manifold to enter the engine.*

1. Introduction

The four-stroke engine was developed by Nicolaus Otto in 1876, and after several years of experimentation on different engines came to a conclusion that the air-fuel mixture be compressed before ignition. It was on the same experimental basis, Otto found that the charge should be compressed, ignited and expanded in the same cylinder. This could be feasible if the operation cycle of the engine was divided into four strokes namely: induction, compression, expansion and exhaust. The Otto- engine, or the four-stroke engine had the following characteristics: Induction of a homogeneous air-fuel mixture into the engine during induction stroke, compression of the charge during the compression stroke, expansion of high-pressure-high-temperature gas during the expansion stroke and evacuation of in-cylinder burned gases from the exhaust valve during the exhaust stroke [1, 2].

A typical internal Combustion (IC) engine consist of the piston head, connecting rod, flywheel, cylinder, crankshaft piston etc. In other words, the piston crown carries the gas pressure, the skirt serves as a bearing against the side thrust of the connecting rod, piston pin connects the piston to the connecting rod, piston ring seals the annular space between the cylinder wall and the piston, connecting rod connects the piston to the crankshaft, thus, reciprocating motion of the piston is converted into rotating motion of the crankshaft [3, 4].

In recent times, automotive industries have shown increased concern on the fuel efficiency, emissions and performance of IC engines, and one of the ways which these factors have been achieved is through the use of Variable Valve Lift (VVL). It is an automotive piston engine technique that varies the height of valve opening in order to improve performance, fuel economy or emissions [5]. This correlates with the findings of [6] where valve lift in diesel engines was observed to influence the air-fuel mixture, emissions and engine combustion performance depending on the valve opening clearance of the air admitted into the combustion chamber.

Several studies have been conducted on valve lift techniques and other IC engine valve related operations, which indicates that valve lift is a major influencing parameter in IC engine. For example, [7] numerically investigated the effect of valve lifts on the emissions and performance of a diesel engine, and found that Gross Indicated Power (GIP), Indicated Mean Effective Pressure (IMEP) and combustion efficiency increased with valve lift opening.

The influence of valve lift in Homogeneous Charge Compression Ignition (HCCI) gasoline engine on the engine performance and emissions were studied by [8]. As the lift of intake valve increased, the air-fuel mixture entering the cylinder increased. When the lift of the intake valve was 5.5 mm, and the lift of the exhaust valve was 3.5 mm, the engine reached a maximum IMEP of 11 bar.

The progress and challenges of unthrottled Miller cycles achieved with a serial-production continuous variable valve train where valve timing is closely linked to valve lift were investigated [9]. Consequently, at low engine load operation the maximum valve lift was lower than 1 mm [10]. This resulted in significant throttling effects for short valve openings, mainly due to very low valve opening and closing velocities. This drawback does not exist for the electro hydraulic valve train, as the valve movement (i.e., the time from fully closed to fully opened and vice versa) is independent of the valve lift or valve timing.

The variable valve timing (VVT) system incorporating a Continuously Variable Cam Phaser (CVCP) for improved fuel economy in a small spark-ignition engine was investigated [11]. The findings revealed that VVT system is a useful tool for optimizing both torque delivery and fuel consumption at part load operation. Furthermore, a weak swirl motion is generated by the intake port at high valve lifts, while a significant swirl level is produced by exhaust backflow through the masked exhaust port at low valve lifts. Late valve closing allows load reduction with significant de-throttling effect but, on the other hand, generates large residual gas fractions. This may be favourable in both NO_x formation and load control, but could lower the combustion rate and the engine thermal efficiency while CO and HC formation could worsen.

Port flow analysis on ICE to determine flow rate and swirl at different valve lift under stationary engine condition was performed [12]. Finite volume method of numerical analysis was employed in solving the continuity, Navier-Stokes and energy equations governing the in-cylinder air-fuel mixture. The result revealed that the mass of air was more concentrated around the valve and inlet port cross-section with swirling motion was observed. Air stream experienced tumbling and turbulence as it flowed downwards the cylinder, which eventually enhanced smooth combustion. From the simulation, it was revealed that mass flow rate of inlet air increased with valve lift.

The effect of variable timing of exhaust valves on SI engine was modelled for improved performance [13]. When Exhaust Valve Closing (EVC) angles reduced to less than 25° before

TDC , there was improvement in the power, BMEP, and BSFC for different engine speeds and reduction in NO and CO emission down to 20° degrees. However, reduction in EVO caused a drop in the engine performance as well as increase in NO and CO emissions.

Port flow analysis was carried out at valve lift of 8 mm using ANSYS R-16 software [14]. The velocity magnitude and mass flow rate were monitored using swirl motion simulated profiles and cut planes. The average angular velocity of the crankshaft was found to be 1315 rpm, with percentage deviation of less than 20%. It was found that the area-weighted average velocity of charge was 11 m/s with corresponding mass flow rate measured as -0.055479 kg/s. The maximum flow rate calculated at 8 mm was 0.005417 kg/s. Intensity of swirl increased along stroke length in the engine cylinder while increase in the swirl number led to uniform radial temperature distribution as well as reduction of in-cylinder flame temperature.

The effect of intake valve lift and closing angle on part load efficiency of a spark ignition engine was investigated [15]. The findings revealed that longer combustion duration resulted from earlier Intake Valve Closing (IVC) angles which led to reduction in turbulence (therefore increasing combustion duration) during combustion, slowing down of flame propagation and lessening the efficiency of heat supply. In-cylinder pressure and temperature levels decreased while heat losses and losses due to incomplete combustion decreased as well. This also caused significant reduction in wall heat losses, blowby, incomplete combustion, as well as the exhaust gas temperature. It was observed that combustion deterioration can be compensated by reduction of heat losses so that reductions of pumping loss during Early Intake Valve Closing (EIVC) can be fully achieved to increase engine's efficiency.

Valve lift in IC engine operation has a number of relationships and effects on the operation parameters, in-cylinder dynamics, operation output, working cycle as well as the overall performance of the engine which has been discussed in many literature including various citations in this study. In actual practice, experimental studies are employed in different engine working scenarios to fully obtain experimental data for each engine parameter. In recent times, computer aided models have been employed in the validation of existing engine parameters which have proven to a reasonable extent that the time, energy and resources invested on experimental procedures can be offset through computer aided modelling and simulations. Hence, the simulation of mass and pressure dynamics of in-cylinder charges at variable valve lift dimensions in four stroke spark ignition engine was conducted in this study using SOLIDWORKS (version 2017) computer aided modelling and simulation techniques.

2. Methodology

The engine and the test environment were modelled with SOLIDWORKS software (2017 version). The engine was a spark ignition (SI) engine assumed to be operating on a four stroke cycle. The engine parameters and boundary conditions were selected from internal combustion engine material library embedded in the software. The model was reduced from a full design to the test design. The full design shows the details of the design but the test prototype showed few components of the engine. The full IC engine model is presented in Figure 1a while Figure 1b shows test prototype of the ICE model with components (piston head, connecting rod, flywheel, cylinder, and crankshaft). The engine parameters and boundary conditions used for the simulation are presented in Table 1.

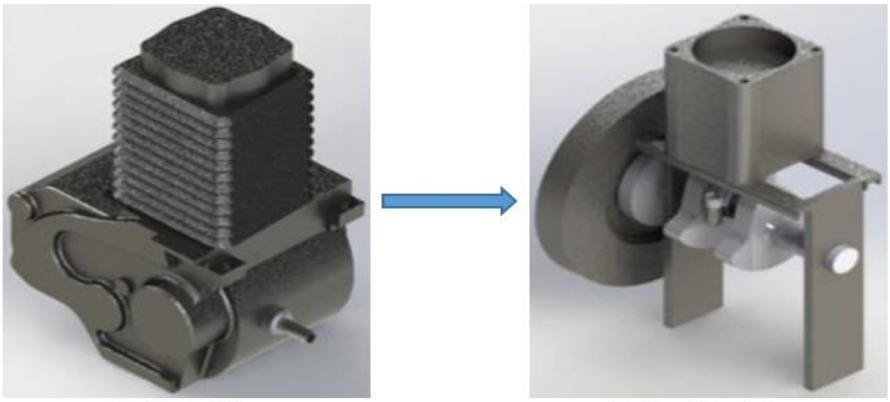

a. Full Model b. Test Prototype

Figure 1: Full ICE engine model and test prototype

Table 1: Engine parameters and boundary conditions for the simulation

Engine parameters	Values	Boundary conditions	Values
Compression Ratio	9.3:1	Initial solid temperature	293.20 K
Stroke	68mm	Air pressure	1.65 bar
Bore	88mm	Air temperature	360 K
Displacement	2500cc	Turbulent Viscosity	1.000 Ns/m^2
Con rod length	122.5	Air to fuel ratio	14.6:1
Swept volume	499.5cm^3	Static Pressure	1.00 bar
Crank shaft bearing	7	Percentage fuel by mass	6.9%
Number of valves	4	Mass flow rate	0.0020 kg/s
Maximum power output	148 bhp or 110 kw	% squish area	10.8
Engine speed	1000-12000 rpm	Specific Dissipation Rate	0.750 m^2/s^3

The partial differential equations governing fluid flows are the known non-linear continuity and Navier-Stokes equations that completely describe the flow of incompressible and Newtonian fluids. For complex flow problems like the in-cylinder flow in spark ignition engines, governing continuity and Navier-Stokes equations are usually applied as closed-form non-linear solutions that consider relevant assumptions, appropriate boundary conditions [12], order of magnitude analysis, and the use of dimensionless parameters. The flow was assumed to be 3-dimensional, incompressible, steady and turbulent. The elements are non-linear and non-uniformly spaced while the analysis was based on a closed cycle with constant amount of working fluid. Applying the boundary conditions, mass and pressure dynamics of the in-cylinder charges at variable valve lift were simulated based on 3D Continuity and Navier Stokes Equations (1, 2 and 3) expressed in Cartesian coordinates.

i. Continuity Equation: A continuity equation expresses a conservation law by equating the net flux over the surface with a loss or gain of material within the surface [16]. Continuity equation in this case is expressed in either integral or differential form in Equation 1.

$$\frac{\partial u}{\partial x}+\frac{\partial u}{\partial y}+\frac{\partial u}{\partial z}=0 \quad (1)$$

ii. Energy Equation: This equation demonstrates that, per unit volume, the change in energy of the fluid moving through a control volume is equal to the rate of heat transferred into the control volume plus the rate of work done by gravity [17] as expressed in Equation 2.

$$\frac{\partial}{\partial t}\left(\rho e+\frac{1}{2}\rho v^2\right)+\frac{\partial}{\partial x}\left(\rho ue+\frac{1}{2}\rho uv^2\right)+\frac{\partial}{\partial y}\left(\rho ve+\frac{1}{2}\rho vv^2\right)+\frac{\partial}{\partial z}\left(\rho we+\frac{1}{2}\rho wv^2\right)=k\left(\frac{\partial^2 T}{\partial x^2}+\frac{\partial^2 T}{\partial y^2}+\frac{\partial^2 T}{\partial xz^2}\right)-\left(u\frac{\partial \rho}{\partial x}+v\frac{\partial \rho}{\partial y}+w\frac{\partial \rho}{\partial z}\right)+\mu\left[u\frac{\partial^2 u}{\partial x^2}+\frac{\partial}{\partial x}\left(v\frac{\partial v}{\partial x}+w\frac{\partial w}{\partial x}\right)+v\frac{\partial^2 u}{\partial y^2}+\frac{\partial}{\partial y}\left(u\frac{\partial u}{\partial y}+w\frac{\partial w}{\partial y}\right)+w\frac{\partial^2 u}{\partial z^2}+\frac{\partial}{\partial z}\left(u\frac{\partial u}{\partial z}+v\frac{\partial v}{\partial z}\right)\right]+2\mu\left[u\frac{\partial^2 u}{\partial x^2}+\frac{\partial u}{dy}\frac{\partial v}{\partial x}+\frac{\partial^2 v}{\partial y^2}+\frac{\partial v}{\partial z}\frac{\partial w}{\partial y}+\frac{\partial^2 w}{\partial z^2}+\frac{\partial w}{\partial x}\frac{\partial u}{\partial z}\right]+\rho ug_x+\rho vg_y+\rho wg_z \quad (2)$$

iii. Momentum (Navier Stokes) Equations: The momentum equation is a statement of Newton's Second Law and relates the sum of the forces acting on an element of fluid to its acceleration or rate of change of momentum. The Newton's second law of motion F = ma forms the basis of the x, y and z momentum equations as represented in Equations 3a-c.

$$\rho\frac{\partial u}{\partial t}+pu\frac{\partial u}{\partial x}+\rho v\frac{\partial u}{\partial y}+\rho w\frac{\partial u}{\partial z}=\rho g_x-\frac{\partial \rho}{\partial x}+\mu\frac{\partial^2 u}{\partial x^2}+\mu\frac{\partial^2 u}{\partial y^2}+\mu\frac{\partial^2 u}{\partial z^2} \quad (3a)$$

$$\rho\frac{\partial v}{\partial t}+pu\frac{\partial v}{\partial x}+\rho v\frac{\partial v}{\partial y}+\rho w\frac{\partial v}{\partial z}=\rho g_y-\frac{\partial \rho}{\partial y}+\mu\frac{\partial^2 v}{\partial x^2}+\mu\frac{\partial^2 v}{\partial y^2}+\mu\frac{\partial^2 v}{\partial z^2} \quad (3b)$$

$$\rho\frac{\partial w}{\partial t}+pu\frac{\partial w}{\partial x}+\rho v\frac{\partial w}{\partial y}+\rho w\frac{\partial w}{\partial z}=\rho g_z-\frac{\partial \rho}{\partial z}+\mu\frac{\partial^2 w}{\partial x^2}+\mu\frac{\partial^2 w}{\partial y^2}+\mu\frac{\partial^2 w}{\partial z^2} \quad (3c)$$

The cylinder volume can be expressed as a function of the crank angle θ and the ratio of the length of the piston rod to the crank. Furthermore, the cylinder volume at any crank angle is given by Equations 4a-b [18]; the piston stroke is given by Equation 5 [19] and the heat transfer per unit area of cylinder wall is given by Equation 6.

$$V=V_c+\frac{V_d}{2}\left(1+\frac{l}{c}-cos\,\theta-\sqrt{\frac{l^2}{c^2}-sin^2\theta}\right) \quad (4a)$$

$$V(\theta)=V_c\left\{1+\frac{r-1}{2}\left\{1-cos\theta+\frac{1}{\varepsilon}[1-(1-\varepsilon^2 sin^2\theta)^{0.5}]\right\}\right\} \quad (4b)$$

$$\varepsilon=\frac{\text{stroke}}{\text{2 x length of connecting rod}} \quad (5)$$

$$\frac{dQ}{A}=h\left(T_{gas}-T_{wall}\right)+C\left(T_{gas}^4-T_{wall}^4\right) \quad (6)$$

Figure 2a represents a typical *p-V* diagram of a Spark Ignition (SI) engine. In the induction stroke, the air-fuel charge is introduced into the cylinder as the piston travels from Top Dead Centre (TDC) to Bottom Dead Centre (BDC). As a result of the piston movement from TDC to BDC, the in-cylinder pressure is reduced to a value in the range of atmospheric pressure (760 mm Hg) [20]. As the piston approaches the bottom of the cylinder, air is channeled through the carburettor, of which the mettered amount of fuel is added to the air. The inlet valve closes at point 2 (see Figure 2a), but this only occur when the piston has traveled midway along the return stroke.

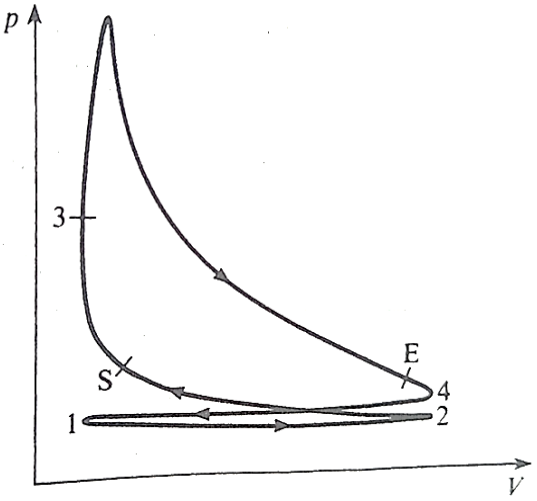

Figure 2: (a) Pressure volume diagram for SI engine

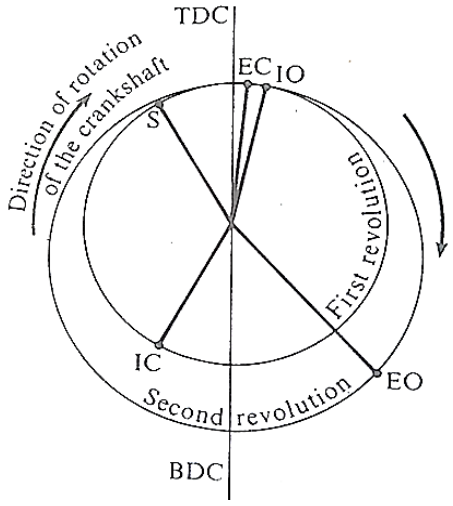

(b) Timing diagram for our-stroke SI engine

With both valves closed, the charge (air-fuel mixture) is compressed by the piston. Therefore, at TDC, the charge occupies the volume over the piston and is known as the clearance volume. The charge is timed accurately to occur at point S (see Figure 2a) which is before TDC. The in-cylinder combustion takes place at almost constant volume, with significant increase in temperature and pressure of the charge during the process. There is an in-cylinder expansion of the hot high-pressure, pushing the piston downwards the cylinder. It appears that the expansion process should proceed to completion at point 4 (see Figure 2a), but the exhaust valve opens somewhere at point E (see Figure 2a) before BDC in order to aid in expulsion of the gaseous products. The pressure at this point is about 3.7 bar or higher [20], and about 60% of the gas is expelled from the exhaust between E and 4 (see Figure 2a) as the in-cylinder pressure drops to almost atmospheric pressure. The returning piston clears the swept volume of exhaust gas and the pressure during this stroke is slightly higher than atmospheric pressure. The aforementioned mixture which is compressed consist of fresh air plus fuel mixture, diluted by a quantity of exhaust gas from the previous cycle [21, 22].

Figure 2b above represents a typical timing diagram for a four stroke SI engine. The angular positions in terms of crank angle positions are indicated in relation to the TDC and BDC positions of the piston [20]. The points on the diagram are highlighted as follows:

i. IO Inlet valve opens: This takes place between 10^o before TDC and 15^o after TDC.
ii. IC Inlet valve closes: The actual position is between 20-40^o after BDC to take advantage of the moment of the rapidly flowing gas.
iii. S Spark: This occurs between 20-40^o before TDC when ignition is more advanced, and at TDC when ignition is fully retarded.
iv. EO Exhaust valve opens: This position occurs at an average value of 50^o before BDC, but it is higher in racing car engines.
v. EC Exhaust valve closes: This occurs between 0-10^o after TDC.

The point indicated represents the normal opening and closing positions for each valve. The time required to open and close the valves implies that each valve will be fully open for a crank angle movement much less than that indicated by the timing diagram. During the downward stroke where the reciprocating piston travels downward from Top Dead Center (TDC) to Bottom Dead Center (BDC) as shown in Figure 3a, the vacuum created in the cylinder is filled by fresh air

entering the combustion chamber through the crankcase. Figure 3b shows the reciprocating piston travelling along the IC engine cylinder.

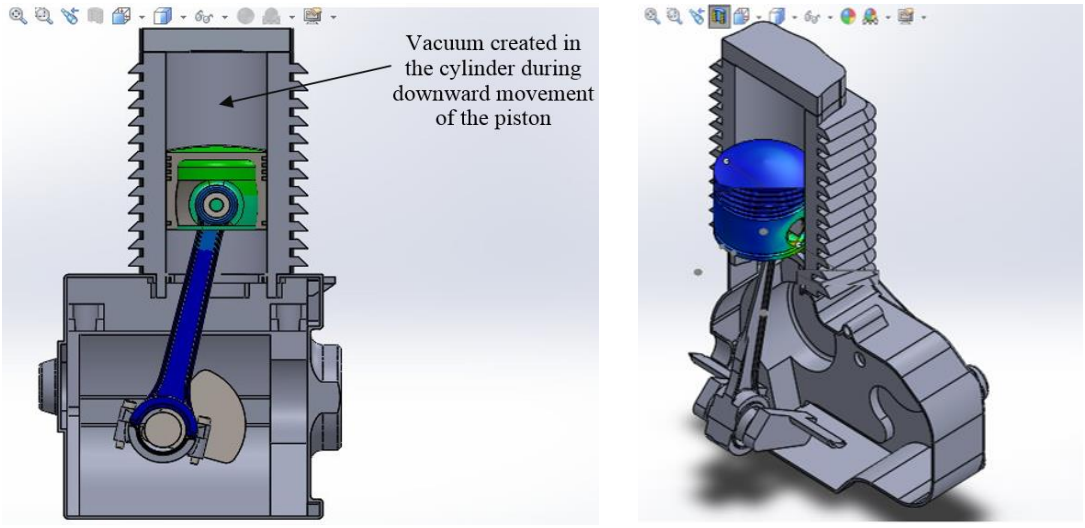

a. **b.**

Figure 3: a. Downward movement of the piston and connecting rod in IC engine cylinder, b. IC engine piston traveling along the cylinder

As the reciprocating piston travels downward, the poppet valve gradually closes due to increased crankcase pressure buildup. As shown in Figure 4, the compressed air-fuel mixture gets expanded in the crankcase prior to the end of the stroke. The reciprocating piston traveling towards the end of the stroke exposes the intake port, thereby, allowing the expanded air-fuel mixture to escape into the main cylinder for compression and expansion at high temperature and pressure before being expelled through the exhaust valve.

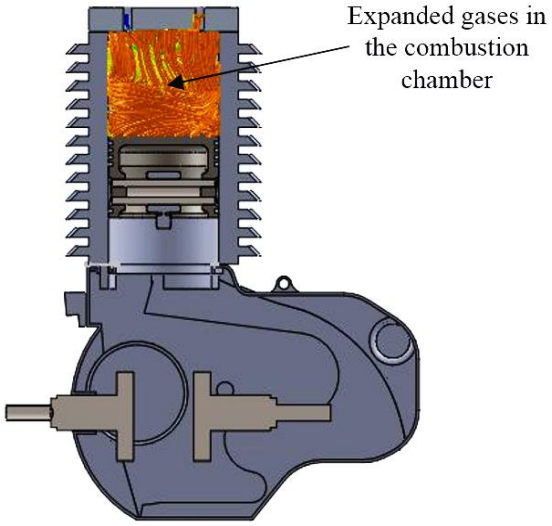

Figure 4: Flow trajectory showing expanded gases in the combustion chamber

3. Results and Discussions

3.1 Mass of charge in the cylinder versus crank speed

Figure 5 shows a plot of the mass of air drawn into the cylinder during intake stroke at different valve lift, from 5mm to 13mm. The intake process was simulated at 1000 rpm engine speed. Careful observation of the plot reveals that at 1000rpm, all valve lift behaved almost the same way and after the intake stroke, the total mass of air drawn into the cylinder was almost equal. However, the mass flow of air is expected to reduce to zero when the intake valve is closed, due to the restriction of compressed air into the cylinder [23]. In this study, valve lift with the highest charge intake was 5mm with a total mass of ingested air as $9.5x10^{-4}kg$ while the valve lift with lowest charge intake was the 13mm lift with a total mass of ingested air being $9.3x10^{-4}kg$. The difference between this two values is quite small and as such, it can be approximated that at low engine speed (below 1000rpm), all valve lift ingest almost the same amount of air during intake stroke [24].

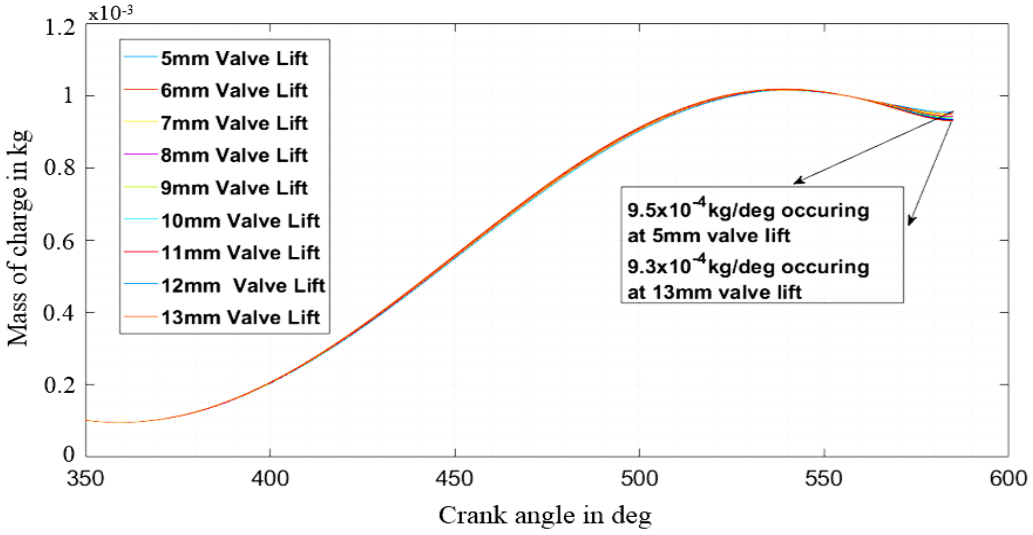

Figure 5: Mass of charge ingested at 1000 rpm for different valve lifts

Figure 6 shows the plot of mass of air drawn into the cylinder during the intake stroke at different valve lift, from 5mm to 13mm. The intake process was simulated at 3000 rpm engine speed. The plot shows that at 3000rpm, all valve lift clearance behaved almost in similar manner, and after the intake stroke, the total mass of air drawn into the cylinder was almost equal. Interestingly, all valve lift ingested the same amount of air at 3000rpm. The value of ingested air was $9.54x10^{-4}kg$ which is slightly higher than the mass ingested at 1000 rpm.

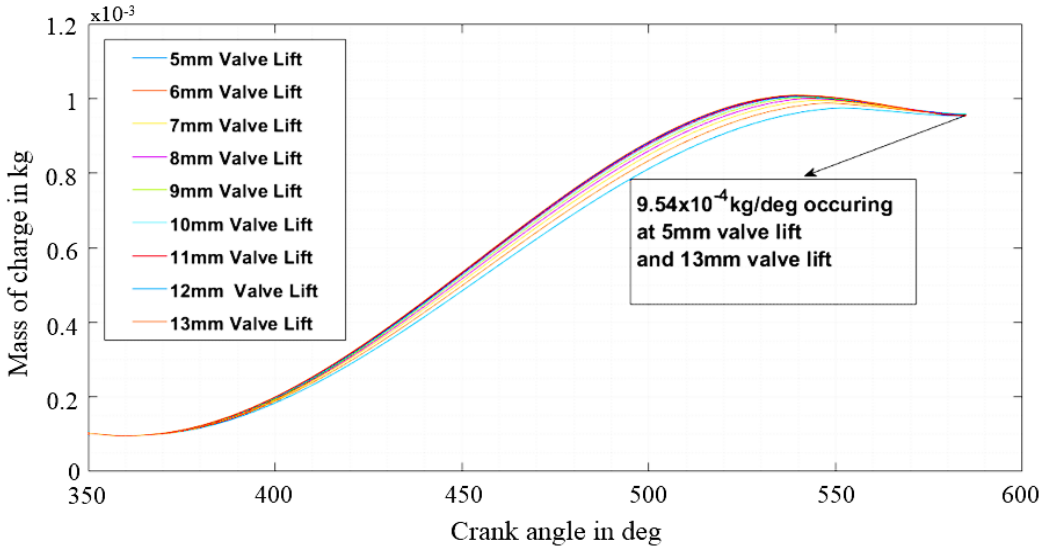

Figure 6: Mass of charge ingested at 3000 rpm for different valve lift

In Figure 7, the highest valve lift ingested the highest amount of air during the intake process. This shows that high engine speed favors larger mass flow intake. Critical observation shows that at 4000rpm, the total mass of charge ingested into the 5mm valve lift is $8.68x10^{-4}kg$ while that of the 13mm valve lift is $8.76x10^{-4}kg$. However, the overall mass of charge recorded as $9.54x10^{-4}kg$ at 3000rpm for valve lift ranging from 5-13mm was higher compared to the same range of valve lift clearance at 4000rpm which indicated a decrease. Therefore, it was observed that at lower engine speed, there is higher mass intake across all variation of valve lift with the lowest valve lift showing the highest charge intake.

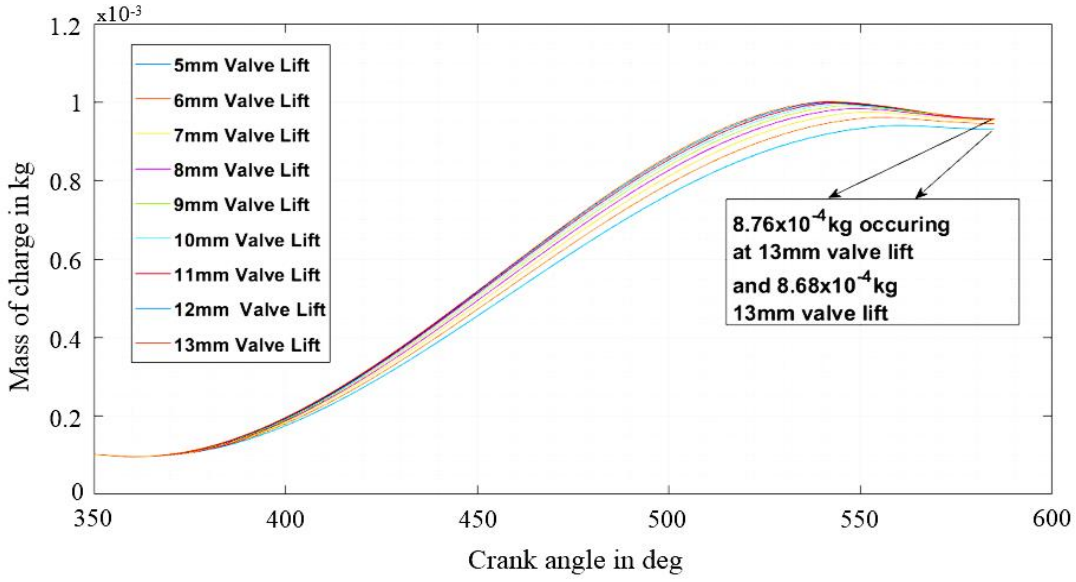

Figure 7: Mass of charge ingested at 4000 rpm for different valve lift

In Figure 8, highest valve lift ingested the highest amount of air during the intake process. This implies that high engine speed favors larger mass flow intake. At 6000rpm, the total mass of charge ingested into the 5mm valve lift was $8.67x10^{-4}kg$ while that of the 13mm valve lift was $9.51x10^{-4}kg$. However, the overall mass of charge increased from 4000rpm to 6000rpm. This

therefore indicates that at lower engine speed, there is higher mass intake across all variation of valve lift, with the lowest valve lift showing the highest charge intake. Moreover, at higher engine speed, the mass intake across all engine is less when compared to low speed [25], but in this case, the higher the valve lift, the more the mass of charge ingested into the engine.

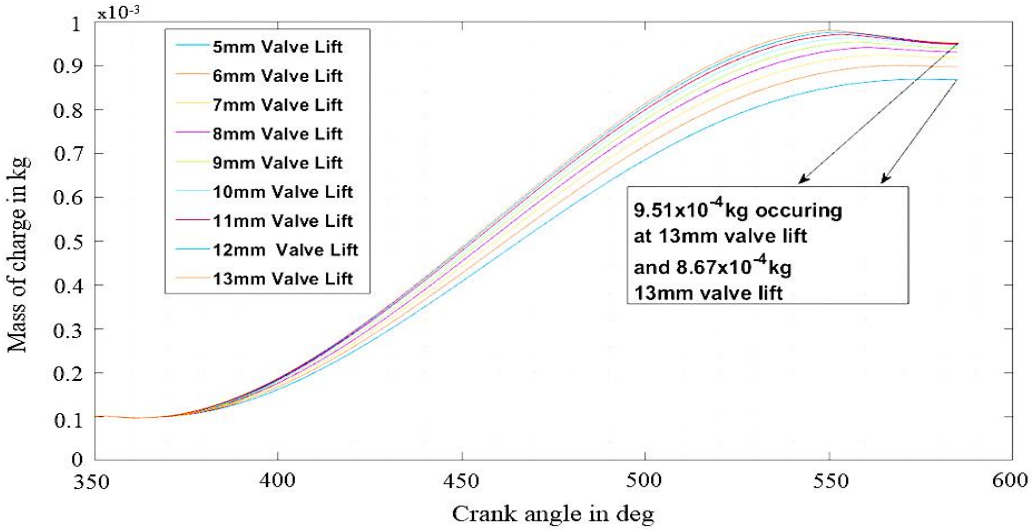

Figure 8: Mass of charge ingested at 6000 rpm for different valve lift

In Figure 9, the highest valve lift ingested the highest amount of air during intake process. This indicates that high engine speed favors larger mass flow intake. A close observation shows that at 9000rpm, the total mass of charge ingested into the engine via 5mm valve lift was $7.77x10^{-4}kg$ while the charge ingested into the engine via 13mm valve lift was $9.23x10^{-4}kg$, indicating that the overall mass of charge decreased from 6000rpm to 9000rpm.

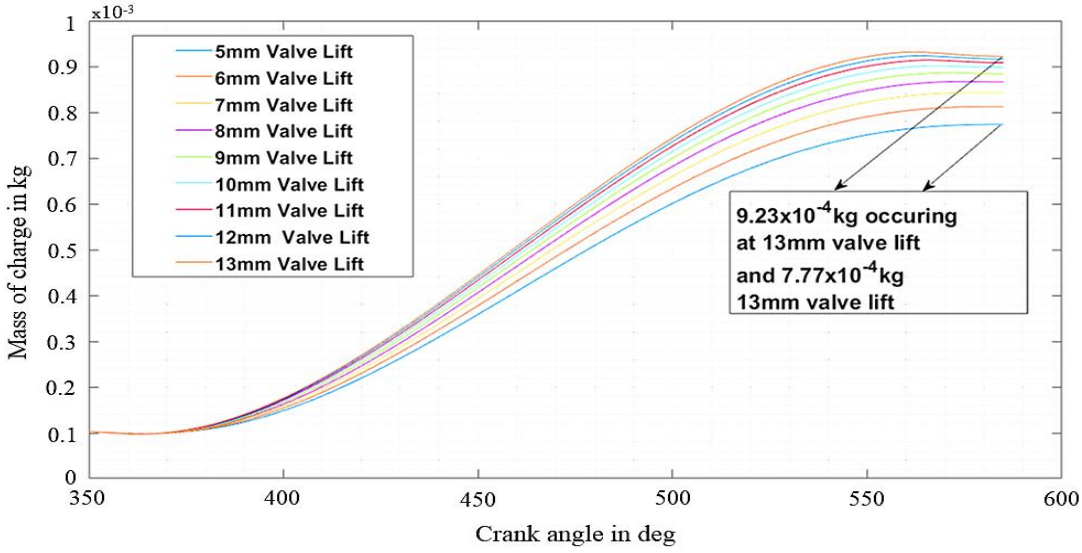

Figure 9: Mass of charge ingested at 9000 rpm for different valve lift

In Figure 10, the highest valve lift ingested the highest amount of air during the intake process. This implies that high engine speed favors larger mass flow intake with higher valve lift, thus, results in higher volumetric efficiency and consequently the power output of the engine increase [26]. Carefully observing the plot shows that at 12000rpm engine speed, the total mass of charge

ingested into the engine cylinder via the 5mm valve lift was $7.02x10^{-4}kg$ while that ingested through 13mm valve lift was $8.78x10^{-4}kg$.

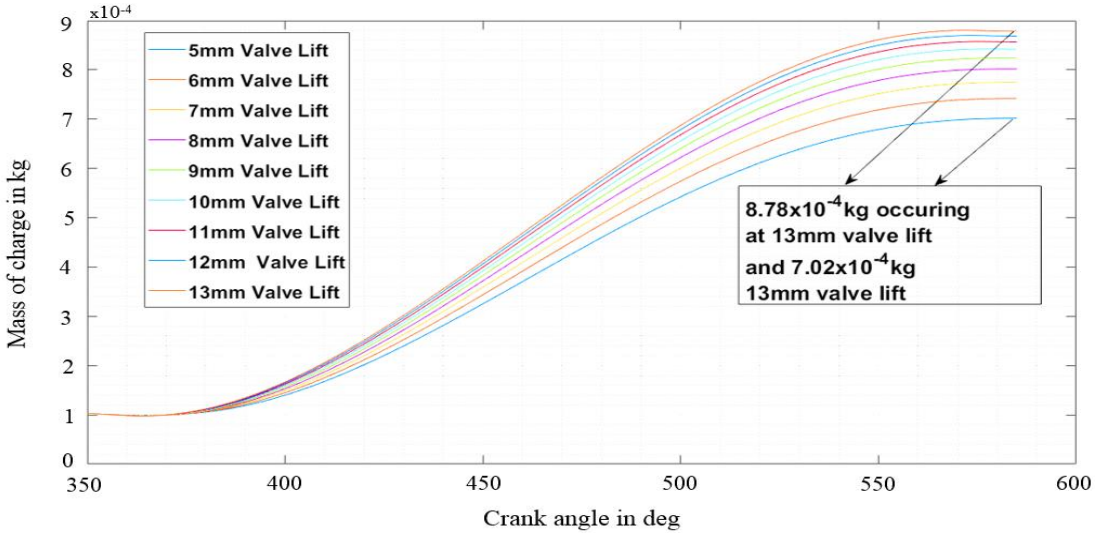

Figure 10: Mass of charge ingested at 12000 rpm for different valve lift

3.2 Pressure of charge in the cylinder versus crank speed

Figure 11 shows a plot of pressure of charge against crank angle during the intake process at various valve lift. The key factor in this plot is the pressure of charge after intake process. The pressure of charge after intake process is very important to IC engine operation, as it improves the performance of the engine. Furthermore, the pressure after intake process can affect the peak pressure of the engine cycle which significantly increase the power output of the engine. This is because, the greater the difference between valve lifts, the higher the level of swirl produced in the cylinder, not taking into account the loss of volumetric efficiency. This results in the increase of power output of the engine [27].

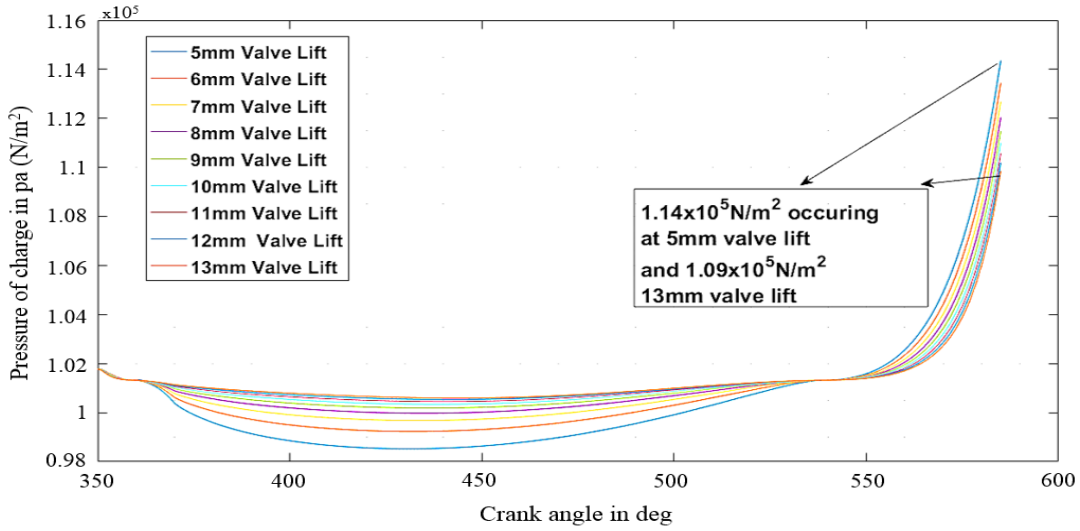

Figure 11: Pressure of charge in the cylinder at 1000 rpm for different valve lift

Careful consideration of the plot (see Figure 11) shows that at 1000 rpm, the valve with lowest valve lift clearance, that is, 5mm valve lift shows the highest pressure after intake process. The reason for this is because of the mass of charge after intake process. At 1000 rpm, 5mm valve lift clearance indicated a pressure of 1.14 bar while 13mm valve lift clearance showed a pressure of 1.09 bar. Figure 12 represents a plot of pressure of charge against crank angle during the intake process at various valve lift clearance. The key factor in this plot is the pressure of charge after intake process.

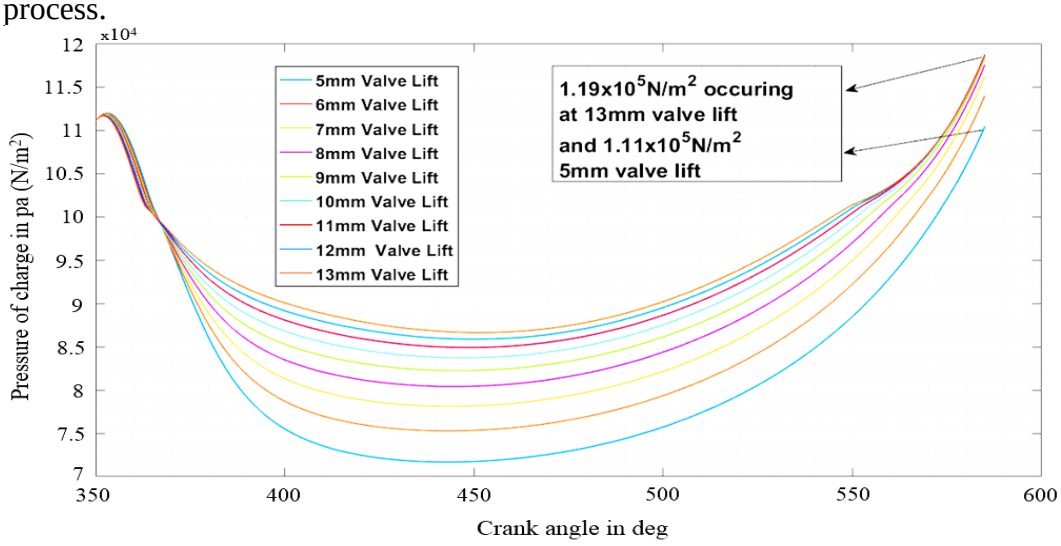

Figure 12: Pressure of charge in the cylinder at 3000 rpm for different valve lift

Careful consideration of the plot in Figure 12, at 3000 rpm, the valve with highest valve lift clearance, that is, the 13mm valve lift showed highest pressure after the intake process. The reason for this is because of the mass of the charge after the intake process. Therefore at 3000 rpm engine speed, 13mm valve lift clearance indicated a pressure of 1.19 *bar* while that of 5mm valve lift clearance showed a pressure of 1.11 *bar*. Figure 13 shows a plot of pressure of charge against crank angle during the intake process at various valve lift clearance ranging from 5-13mm at engine speed of 4000 rpm. The pressure after the intake process is observed to affects the peak pressure of the engine cycle which significantly increased the power output of the engine.

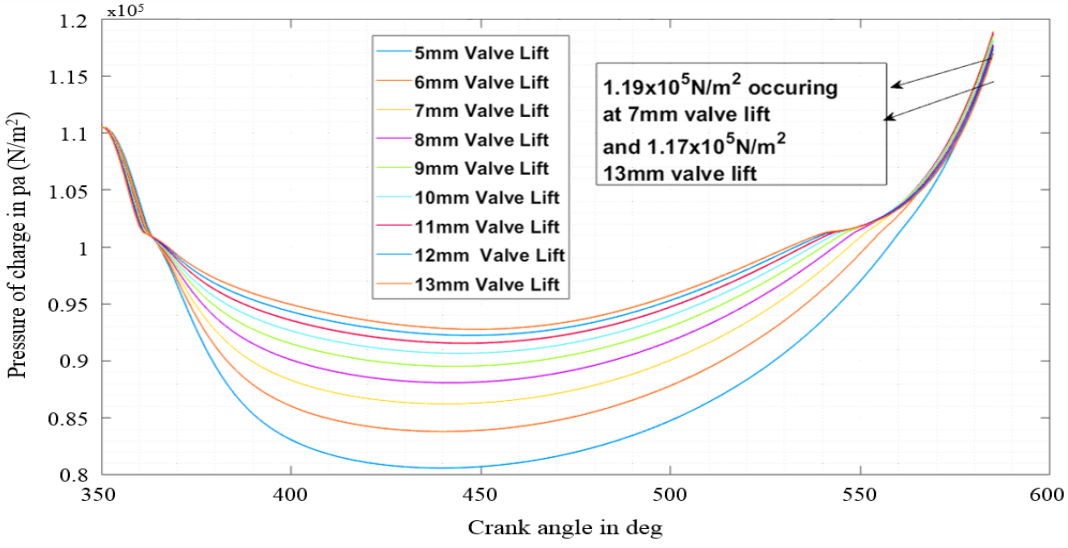

Figure 13: Pressure of charge in the cylinder at 4000 rpm for different valve lift

Careful consideration of the plot in Figure 13, at engine speed of 4000 rpm, the pressure after intake process is the same for all valve lift. This is because the mass of charge drawn into the cylinder at 4000 rpm is approximately the same for all value of valve lift. Figure 14 shows a plot of pressure of charge against crank angle during intake process for various valve lift clearance ranging from 5-13mm at engine speed of 6000rpm. Also, the pressure after the intake process affects the peak pressure of the engine cycle which significantly increases the power output of the engine [28].

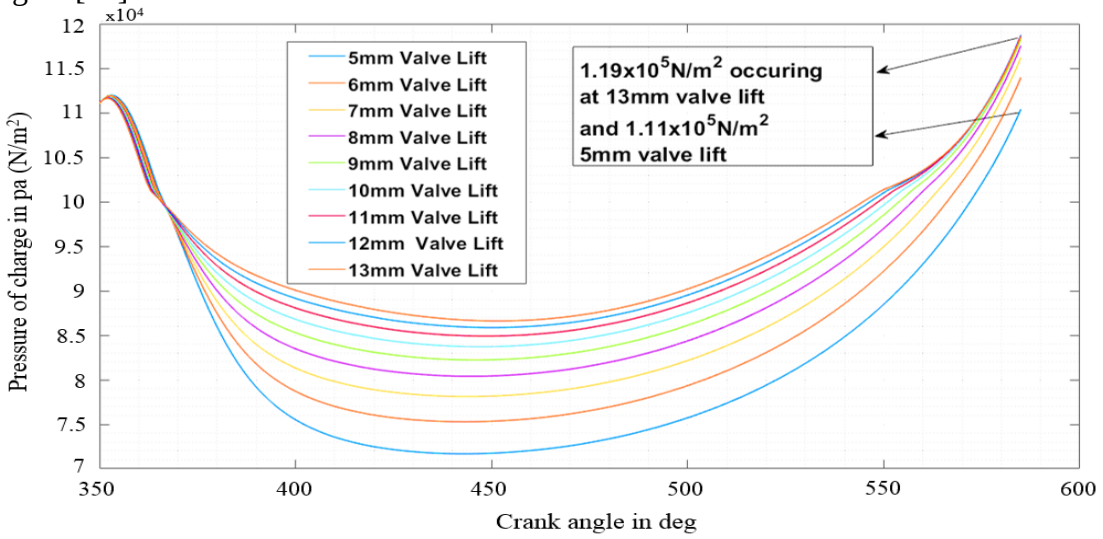

Figure 14: Pressure of charge in the cylinder at 6000 rpm for different valve lift

Careful consideration of the plot in Figure 14, at engine speed of 6000 rpm, the valve with the highest valve lift clearance, that is, the 13mm indicates the highest pressure after the intake process. At 6000 rpm, the 13mm valve lift showed a pressure of 1.19 bar while the 5mm valve lift showed a pressure of 1.11 bar. This indicates that in-cylinder pressure increases as the valve lift opening clearance increase. Figure 15 shows a plot of pressure of charge against crank angle during the intake process for various valve lift ranging from 5-13mm at engine speed of 9000rpm. Also, the pressure after the intake process is observed to affects the peak pressure of the engine cycle which significantly increased the power output of the engine. This correlates with the findings of [23] which clearly revealed that increasing in-cylinder pressure improves the torque [29] and power output but causes reduction in terms of the energy efficiency.

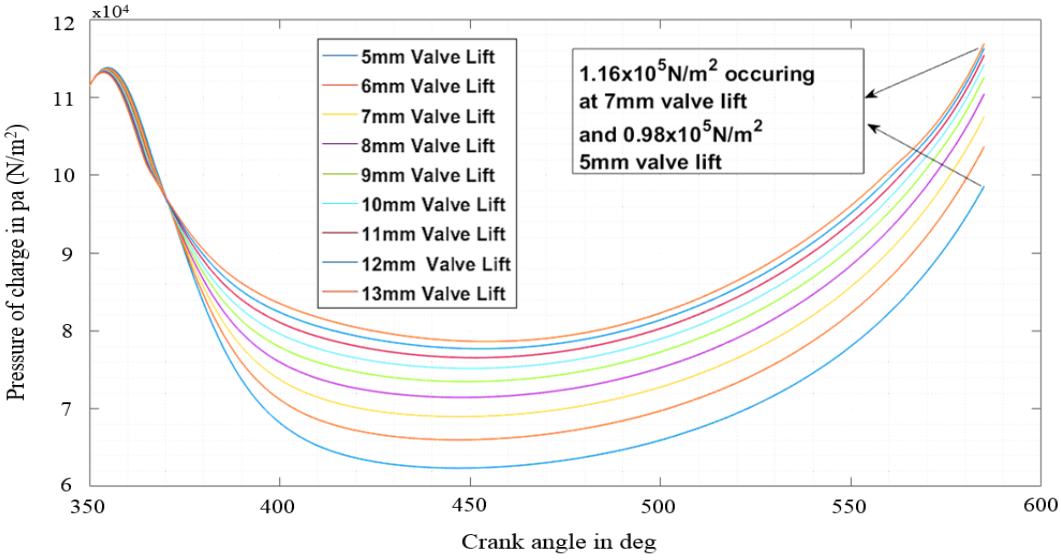

Figure 15: Pressure of charge in the cylinder at 9000 rpm for different valve lift

Careful consideration of the plot in Figure 15 at engine speed of 9000rpm, valve with the highest valve lift clearance which in this case is 13mm indicated highest pressure after the intake process. At 9000 rpm, the 13mm valve lift showed a pressure of 1.16 bar while the 5mm valve lift showed a pressure of 0.98 bar. Figure 16 shows a plot of pressure of charge against crank angle during the intake process at various valve lift ranging from 5-13mm at engine speed of 12000rpm. Careful consideration of the plot reveals that at engine speed of 12000 rpm, the valve with the highest valve lift which in this case is 13mm showed the highest pressure after the intake process. Therefore at engine speed of 12000 rpm, the 13mm valve lift showed a pressure of 1.12 bar while that of 5mm valve lift showed a pressure of 0.89 bar. However, studies have shown that increasing the valve lift opening clearance can cause increase in the amount of fresh charges (air-fuel mixture) entering the cylinder [30, 31].

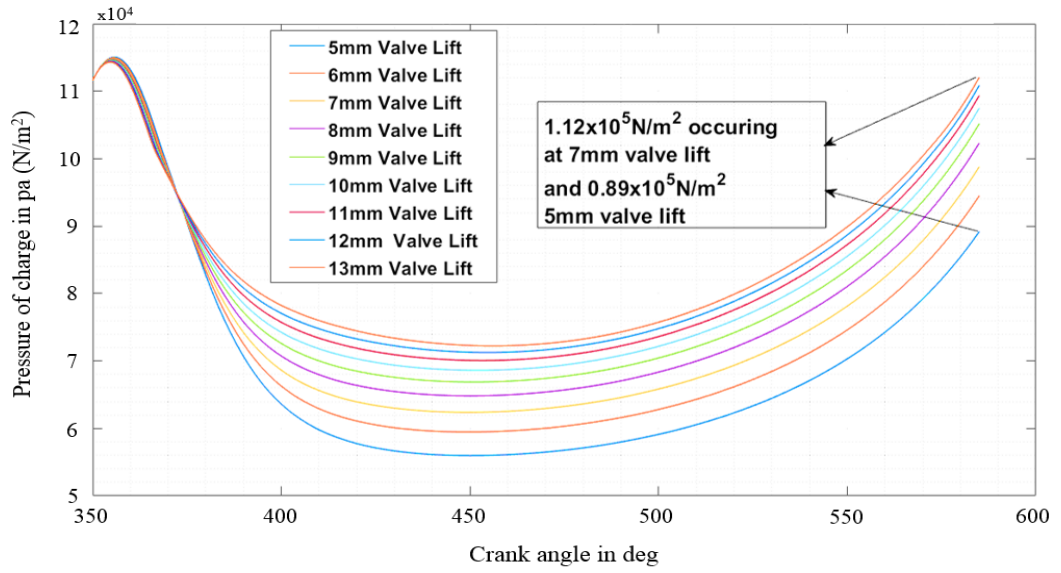

Figure 16: Pressure of charge in the cylinder at 12000 rpm for different valve lift

4. Conclusion

This paper presents a numerical analysis of an IC engine. The intake valve lift clearance affects various engine parameters which are not limited to; pressure after the intake stroke, mass of the charge induced during intake stroke, temperature of charge after intake stroke, mass flow rate through the engine during intake stroke and more importantly the volumetric efficiency of the engine. From the analysis of the results obtained after simulation, it was observed that at lower engine speed, the engine performance improved when operated at valve lift below 6 mm. This is because at lower engine speed, there is enough time for the charge to enter the engine cylinder for effective compression and expansion which consequently influence the pressure, temperature, and mass of the intake charge. At higher engine speed, the engine performed better when operated at valve lift greater than 9mm. The reason for this behavior is that at high engine speed, there is less time for the charge to be drawn into the engine and only higher valve lift can allow high mass flow rate through the engine. However at higher valve lift clearance, the in-cylinder high-temperature-high-pressure can cause losses to the charge in the cylinder as well as the intake point, thereby, resulting in low compression, low engine efficiency, low power output and vice versa. It should be noted that the percentage of losses at every intake cycle depends on the integrity of the engine. Hence, VVT is can be employed to control the timing of valve lift event for improved performance, fuel economy and emissions. Furthermore, proper maintenance, repairs and replacement of all faulty engine parts should be ensured for the engine to meet desired performance in its duty cycle.

Nomenclature

BMEP	Break mean effective pressure
BSFC	Break-specific fuel consumption
V_c	Clearance volume
V_d	Displacement volume
r	Compression ratio
ε	Piston stroke
EVC	Exhaust Valve Closing
EVO	Exhaust valve open
EIVC	Early intake valve closing
GIP	Gross indicated power
IMEP	Indicated mean effective pressure
IC	Internal combustion
ICE	Internal combustion engine
IVC	Intake valve closing
∂_t	Tangential velocity
HCCI	Homogeneous Charge Compression Ignition
μ	Mixture viscosity
CVCP	Continuously Variable Cam Phaser
z	Radial coordinate
u	Axial velocity
w	Swirl velocity
dQ/A	Heat transfer per unit area
C	Annand closed cycle coefficient

SI	Spark ignition
TDC	Top dead centre
BDC	Bottom dead centre
VVL	Variable valve lift
VVT	Variable valve timing
3D	Three (3) dimension

References

[1] B. Johansson and F. Soderberg (1996). The Effect of Valve Strategy on In-Cylinder Flow and Combustion. SAE paper 960582. The SAE Congress and Exposition Feb. Detroit, Michigan.
[2] F. Soderberg (1998). A Study of Fluid Flow and Combustion with Variable Valve Timing. Lund Institute of Technology, Sweden, ISRN: LUTMDN/TMHT-98/7029-SE.
[3] K. S. Balahari, V. M. Aezhisai, M. Arunkumar and A. Haripraveen (2017). Design and analysis of an IC engine piston using composite material. Eur. J. of Adv. in Eng. and Tech, Vol.4(3), pp.209-215.
[4] I. B. Owunna and A. E. Ikpe (2020). Design analysis of reciprocating piston for single cylinder internal combustion engine. Int. J. of Auto. Sci. and Tech, Vol.4(2), pp.30-39.
[5] N. X. Khoa and O. Lim (2021). A Study to Investigate the Effect of Valve Mechanisms on Exhaust Residual Gas and Effective Release Energy of a Motorcycle Engine. Energies, Vol.14, pp.1-14.
[6] S. M. Begg, M. P. Hindle, T. Cowell and O. Heikal (2009). Low intake valve lift in a port fuel-injected engine. Energy, Vol.34(12), pp.2042-2050.
[7] K. Bayramoglu, S. Yilmaz and K. D. Kaya (2019). Numerical Investigation of Valve Lifts Effects on Performance and Emissions in Diesel Engine. Int. J. of Glo. Warming, Vol.8(3-4), pp.287-303.
[8] C. Cinar, A. Uyumaz, H. Solmaz, and T. Topgul (2015). Effects of valve lift on the combustion and emissions of a HCCI gasoline engine. Energy Conv. Mang. Vol.94, pp.159-168.
[9] H. Unger, C. Schwarz, J. Schneider and K. Koch (2008). The Valvetronic: Experience from Seven Years of Mass Production and a Discussion of Future Prospects. Springer MTZ Worldwide, 69(7-8), 30-37.
[10] C. Luttermann, E. Schünemann and N. Klauer (2010). Enhanced VALVETRONIC Technology for Meeting SULEV Emission Requirements. SAE Technical Paper 2006-01-0849, 1-7.
[11] G. Fontana, and E. Galloni (2009). Variable valve timing for fuel economy improvement in a small spark-ignition engine. App. Energy, Vol.86, pp.96-105.
[12] S. M. G. Akele, C. Aganama, E. Emeka, Y. Abudu-Mimini, S. Umukoro and R. Okonkwo, R. (2020). CFD Port Flow Simulation of Air Flow Rate in Spark Ignition Engine. Int. J. of Eng. and Mang. Res, Vol.10(6), pp.87-95.
[13] O. H. M. Ghazal, Y. S. H. Najjar and K. J. M. Al-Khishali (2013). Modelling the Effect of Variable Timing of the Exhaust Valves on SI Engine Emissions for Greener Vehicles. Energy and Pow. Eng. Vol.5, pp. 181-189.
[14] A. E. Ikpe, I. B. Owunna and P. O. John (2021). Port Flow Simulation and In-cylinder Swirl Motion Characteristic Effects in Internal Combustion Engine Duty Cycle. App. of Modl. and Sim. Vol.5, pp.102-114.
[15] M. Balmelli, N. Zsiga, L. Merotto and P. Soltic (2020). Effect of the Intake Valve Lift and Closing Angle on Part Load Efficiency of a Spark Ignition Engine. Energies, Vol.13, pp. 2-16.
[16] M. Towhiduzzaman (2016). Performance Analysis of Continuity Equation and Its Applications. Eur J. of Eng. Res and Sci, 1(5), 40-43.
[17] Movva, V. S. (2004). Simulation of Fluid Flow in Internal Combustion Engine using Wave Action Simulation. Thesis, Texas Tech University.
[18] S. Ramachandran (2009). Rapid Thermodynamic Simulation Model of an Internal Combustion Engine on Alternate Fuels. Proc. of the Int. Multi-conference of Eng. and Comp. Sci., Hong Kong, Vol.2, pp.18-20.
[19] C. R. Ferguson and A T. Kirkpatrick (2000). Internal Combustion Engine: Applied Thermosciences, 2nd Edition, New York, John Willey and Sons, ISBN: 0471356174.
[20] T. D. Eastop and A. McConkey (1993). Applied Thermodynamics for Engineering Technologies. Fifth Edition, Pearson Education Limited, ISBN: 0-582-09193-4.
[21] M. H. A. Rosli, M. R. Hanipah and M. Kettner (2019). The tuning of a small four-stroke spark ignition engine for flexible valve timings through numerical approach. MATEC Web of Conferences, 255(04004), PP.1-10.

[22] A. E. Ikpe and I. B. Owunna (2020). A 3D modelling of the in-cylinder combustion dynamics of two stroke internal combustion engine in its service condition. Nig. J. of Tech. Vol.39(1), pp.161-172.
[23] Q. Yu, Y. Shi and M. Cai (2014). Working Characteristics of Variable Intake Valve in Compressed Air Engine. The Scientific Wld. J., 2014, 1-9.
[24] A. Yazdani (2016). Air Charge Estimation for an SI Engine using In-cylinder Pressure Sensor. Thesis, Michigan Technological University.
[25] M. Balmelli, N. Zsiga, L. Merotto and P. Soltic (2020). Effect of Intake Valve Lift and Closing Angle on Part Load Efficiency of a Spark Ignition Engine. Energies, 13(1682), 2-16.
[26] V. K. Sharma, M. Mohan and C. Mouli (2017). Effect of Intake Swirl on the Performance of Single Cylinder Direct Injection Diesel Engine. IOP Conference Series: Mat. Sci. and Eng. 263(062077), 1-8.
[27] D. E. Ramajo and N. M. Nigro (2010). In-cylinder Flow CFD Analysis of a Four-valve Spark Ignition Engine: Comparison between Steady and Dynamic Test. J. of Eng. for Gas Turbine and Pow, 132, 1-10.
[28] I. B. wunna and A. E. Ikpe (2021) Comparative Analysis of Four Stroke and Six Stroke Internal Combustion Renault Engine Efficiency Using Matlab Simulation Tool. Nig. J. of Eng., 28(3), 2705-3954.
[29] M. D. Nora, T. Lanzanova and H. Zhoa (2016). Effects of Valve Timing, Valve Lift and Exhaust backpressure on Performance and Gas Exchanging of a Two Stroke GDI Engine with Overhead Valves. Energy. Convers. Manag, 123, 71-83.
[30] C. Cinar, A, Uyumaz, H. Solmaz and T. Topgul (2015). Effects of Valve Lift on Combustion and Emissions of a HCCI Gasoline Engine. Energy. Convers. Manag, 94, 159-168.
[31] N. X. Khoa and O. Lim (2021). A Study to Investigate the Effect of Valve Lift Mechanisms on Exhaust Residual Gas and Effective Release Energy of a Motorcycle Engine. Energies, 14, (5564), 2-14.